

1 All-flavor Multi-Channel Analysis of the 2 Astrophysical Neutrino Spectrum with IceCube

The IceCube Collaboration[†]

[†] http://icecube.wisc.edu/collaboration/authors/icrc17_icecube

E-mail: cweaver@icecube.wisc.edu, nwandkowsky@icecube.wisc.edu

The spectral shape and flavor composition of the high-energy astrophysical neutrino flux can contain important information about the sources and processes which produce it. The IceCube Neutrino Observatory has previously demonstrated the ability to observe neutrinos of all flavors by selecting events which interact within the detector volume. Sensitivity to charged current muon neutrino interactions in or close to the detector has also been shown by selecting muon track events whose directions indicate passage through the Earth. We present an updated analysis of starting events using 6 years of IceCube data taken from 2010–2016 focusing on energies from the PeV region down to 1 TeV, far below the threshold of the original data sample used in the initial discovery of the astrophysical flux. Astrophysical neutrinos remain the dominant component in the southern sky down to 10 TeV. We then also perform a unified analysis of the flavor and spectrum implications of this sample when combined with the recently published data on ν_μ induced muon tracks as well as recent work to identify candidate ν_τ events.

Corresponding authors: N. Wandkowsky¹, C. Weaver^{*2}

¹*Dept. of Physics and Wisconsin IceCube Particle Astrophysics Center, University of Wisconsin, Madison, WI 53706, USA*

²*Dept. of Physics, University of Alberta, Edmonton, Alberta, Canada T6G 2E1*

*35th International Cosmic Ray Conference — ICRC2017
10–20 July, 2017
Bexco, Busan, Korea*

*Speaker.

3 1. Introduction

4 Neutrinos have the potential to provide important information for understanding the mecha-
5 nisms of energetic astrophysical objects and their relationship to cosmic rays. With the successful
6 observation of a diffuse flux of astrophysical neutrinos, both in the form of events starting within
7 a fiducial volume of a detector [2, 5] and events with Earth-crossing directions [3], a major goal is
8 now to determine the properties of this flux in the greatest possible detail. This can be pursued both
9 by extending the selection of neutrino candidate events to capture as many astrophysical neutrinos
10 as possible, including substantial numbers of atmospheric neutrinos to ensure that backgrounds are
11 well understood, and by combining different selection techniques into more thoroughly integrated
12 analyses of the total spectrum. Here, we discuss both improvement of the selection of starting
13 events in the IceCube detector and a new iteration of a global analysis of the neutrino flux utilizing
14 the latest high statistics datasets and event observables.

15 2. Starting Event Selection

16 Identifying of neutrino candidate events in IceCube by utilizing a division of the detector into
17 an internal fiducial volume and a surrounding veto layer has proven highly successful in obtaining
18 a high purity sample of neutrinos. Additionally, a large fraction of these neutrinos are expected to
19 be of astrophysical origin. Because the development of this technique was spurred by the observa-
20 tion of events in the PeV range of energy [1], the initial focus was on these high energies. Lower
21 energies, where backgrounds produced by cosmic ray air showers pose a greater challenge, were
22 left unexplored. Subsequently, the veto technique has been extended, using additional event recon-
23 struction information and dynamic scaling of the boundary between the fiducial and veto volumes.
24 This lowers the selection threshold to events depositing around 1 TeV of energy [5], but thus far
25 this enhanced technique has been applied to only two years of IceCube data. This new version of
26 the selection further optimizes this technique to maximize efficiency. A splitting algorithm, using
27 a form of agglomerative hierarchical clustering, is applied to each recorded event to attempt to
28 separate unrelated, coincident events in the detector, with a success rate of about 75%. The ‘outer
29 layer’ veto criterion as in [1] is then applied, rejecting all events which are observed to have more
30 than three detected photons in the veto region. The splitting reduces the fraction of events falsely
31 vetoed due to coincident events and makes this selection a superset of the selection of [1] for events
32 which yield at least 6000 photoelectrons detected.

33 To provide efficient background rejection for lower energy events, following the technique of
34 [5], a more sensitive veto for incoming particle tracks is then applied, relying on the reconstruction
35 of the location of the interaction vertex (or a major energy deposition within the event) followed
36 by a search over downward directions for detected photons whose timing is consistent with an in-
37 coming particle. Any event with more than two such veto photons is discarded. This same veto
38 method is also applied in reverse to detect tracks directed outward and upward from the recon-
39 structed event vertex, as such a track is a strong indication that the event is a charged-current ν_μ
40 interaction. Events with at least 10 photoelectrons consistent with an upward track are immediately
41 preserved. Finally, events which produce lower observed numbers of photons are subjected to a
42 volume cut, more stringent with decreasing energy, increasing the amount of veto path length which

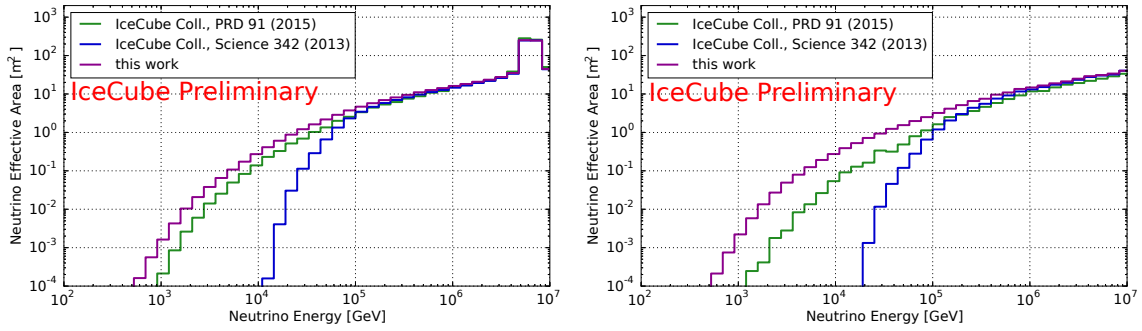


Figure 1: Effective area of the starting event selection for ν_e (left panel) and ν_μ (right panel) is shown in purple, compared to the effective areas from [1] in blue and [5] in green. All effective areas are averaged over neutrinos and antineutrinos. The effective area for ν_τ is quite similar to that for ν_e except for the lack of the resonance feature at several PeV.

43 a background muon would have to traverse unseen. An important change with respect to [5] is that
 44 to avoid discrimination against starting charged-current ν_μ interactions that produce more clearly
 45 track-like events, a broader selection using data from IceCube’s first-level ‘online’ filters gives a
 46 considerable increase in the efficiency with which these events are selected. Fig. 1 shows the result-
 47 ing effective area for this selection compared to the previous veto-based selections. This selection
 48 delivers higher efficiency for all event topologies, particularly a factor ~ 2 for ν_μ at around 100
 49 TeV to a factor of ~ 8 at around 10 TeV. Further, it is intended that this selection will be applied to
 50 the same six years of IceCube data as in [4], three times the data-taking period covered by [5], and
 51 it is anticipated that this will continue to be extended in future as new data become available.

52 As this selection collects events of both track-like and cascade-like topologies, it is useful to
 53 distinguish between the two. Events with 10 photoelectrons of out-going light attributable to an
 54 up-going track are naturally classified as track-like. Otherwise, each event is reconstructed using
 55 both track and cascade hypotheses, and the average distance of the modules which observed light
 56 to the best fit particles is computed. This provides a useful observable because true track events
 57 tend to have light at large distances from the best fit cascade hypothesis. Finally, an unfolding
 58 of the probable energy depositions within each event is performed, using both a single, point-like
 59 deposition hypothesis, representing a cascade, and a hypothesis of a linear collection of deposi-
 60 tions, representing a muon. For bright events with more than 6000 photoelectrons detected, if the
 61 linear unfolding has non-negligible depositions located more than 500 meters apart, the event is
 62 considered track-like. Likewise, bright events for which the observed charge associated with the
 63 linear unfolding is larger than the observed charge associated with the single point unfolding are
 64 classified as tracks; other bright events are classified as cascades. For dimmer events, if at least 1.5
 65 photoelectrons of out-going charge are detected the event is classified as track-like, and otherwise
 66 it is considered cascade-like. Based on Monte-Carlo simulations, more than 98% of truly cascade-
 67 like events are correctly classified as such. Figure 2 shows the success rate for classification of
 68 true ν_μ charged-current events, which is above 80% when averaged over energy and position for
 69 an astrophysical spectrum $\propto E^{-2.5}$. Misclassified ν_μ charged-current events are expected to make
 70 up 30% of the cascade-like category from a conventional atmospheric spectrum, but only 5% from
 71 a spectrum $\propto E^{-2.5}$.

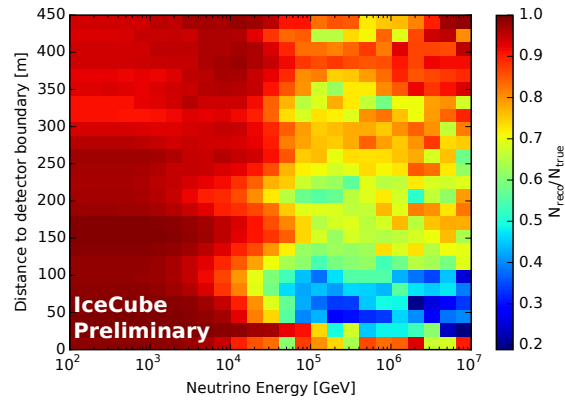


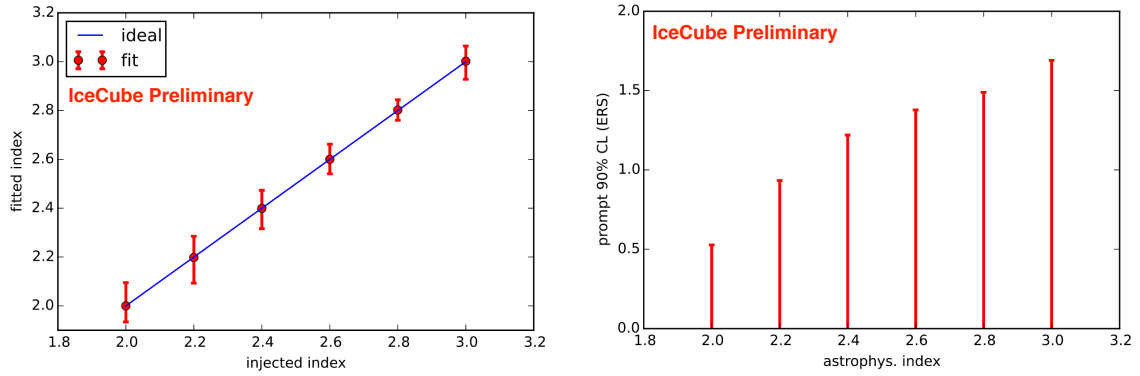
Figure 2: Probability that starting ν_μ charged-current events are correctly classified as track-like. Since the selection requires lower energy events to start deeper inside the detector, these are more likely to be correctly classified due to having an observation of the out-going track.

72 3. Starting Event Analysis

73 A new sample of starting neutrino events provides opportunities for studying the diffuse neu-
 74 trino flux. These data will be analyzed using a binned, forward-folding maximum likelihood fit to a
 75 set of parameterized models, as in many previous analyses. Three observables are used in the likeli-
 76 hood fit. The reconstructed event energy gives access to spectral shape information. Reconstructed
 77 event direction (zenith angle in detector coordinates) carries information about atmospheric origin
 78 due to non-uniform production of atmospheric neutrinos from light meson decays (‘conventional’
 79 atmospheric neutrinos) and the self-veto effect of muons produced in the same air showers. Last,
 80 the assessed event topology gives the analysis a degree of flavor sensitivity. In terms of the model
 81 which will be used to fit the data, four spectral components will be included: the conventional atmo-
 82 spheric neutrinos, ‘prompt’ atmospheric neutrinos (from short-lived particle decays), penetrating
 83 muons from cosmic ray air showers, and a diffuse, astrophysical flux of neutrinos.

84 The three atmospheric components are each allowed to vary in normalization. No prior is
 85 placed on the normalization of the conventional component as it is expected to be well constrained
 86 by the data, the prompt component is given a gaussian prior centered at zero with a width of 2.3
 87 times the ERS model normalization [6] following the result obtained in [7], and the penetrating
 88 muons are given a prior centered at the rate estimated from a tagged sample of experimental back-
 89 ground events with a width of 50% [2]. These priors are expected to have only weak influence on
 90 the final result. In addition, to treat systematic uncertainties arising from the primary cosmic ray
 91 flux and from the modeling of hadronic interactions in air showers, parameters will be included for
 92 variation in the effective cosmic ray spectral index and the relative production rates of kaons with
 93 respect to pions in air showers. Systematic treatment of uncertainties in the response of the detector
 94 itself will also be addressed, specifically the absolute optical efficiency of the detector, the optical
 95 properties of the ice surrounding the modules, and the scattering of the ice which was melted and
 96 refrozen during installation of the instrumentation.

97 For the purposes of this study, the astrophysical neutrinos are assumed to be isotropic and
 98 have equal contributions from all neutrino flavors. The base model to be tested will be a single



(a) 68% sensitivity to spectral index of a single astrophysical power law flux

(b) 90% sensitivity to a prompt atmospheric neutrino flux assuming the spectrum of ERS [6] relative to the normalization of that model

Figure 3: Median projected sensitivity of the starting event analysis to model parameters assuming 6 years of data. A variety of spectral indices are considered to ensure that the analysis performs well for any possible input.

99 power law with variable normalization and spectral index. Additionally, a set of more advanced
 100 astrophysical models will be tested, including an exponential spectral cutoff, a second power law
 101 component, and the combination of both of these additions. Finally, the flavor composition of the
 102 astrophysical flux will be tested by allowing the normalization associated with each neutrino flavor
 103 to float independently in the fit, although all three flavors will be assumed to have the same spectral
 104 shape. Fig. 3 shows the expected median sensitivity of this analysis for two of the parameters
 105 considered over a variety of possible true astrophysical fluxes with different spectral indices and
 106 normalizations chosen to be consistent with the observations of [2]. This analysis is expected to
 107 have good resolution of the spectral index of a single astrophysical power law component, but the
 108 sensitivity to a prompt atmospheric component is expected to be limited by the strength (and also
 109 uncertainty) of the astrophysical flux, particularly if that flux is relatively soft.

110 4. Global Flavor Analysis

111 Beyond analyzing the more complete dataset of starting events, it is desirable to unify the
 112 analysis of all types of neutrino data observed by IceCube. This type of analysis has been per-
 113 formed previously [8]; the purpose of this new iteration is to use newer datasets and observables
 114 which have become available. Particularly complementary to the starting event sample is the high
 115 statistics sample of muons from Earth crossing neutrinos analyzed previously [3], and continues
 116 to be extended to newer data [10]. While the starting event selection is most sensitive to the as-
 117 trophysical neutrino flux in the southern portion of the sky, as this is the angular region in which
 118 atmospheric neutrinos are most strongly self-vetoed, the Earth-crossing neutrinos are most sen-
 119 sitive to high energy events near the horizon. Consisting almost entirely of ν_μ charged-current
 120 events, the Earth-crossing sample has essentially no flavor sensitivity on its own, but provides a
 121 strong constraint on the ν_μ portion of the astrophysical flux. The starting event sample constrains
 122 the combined flux of ν_e and ν_τ in addition to contributing to the ν_μ measurement. In fact, it is

123 possible to do better than treating ν_e and ν_τ as equivalent cascade-like events by using specialized
124 reconstruction for double cascade events resulting from ν_τ charged-current interactions as detailed
125 in [9]. Some care must be taken when combining these three datasets to avoid double counting
126 events. Since the ν_τ component is the least well constrained, the τ observables only function well
127 for high energy events, and the starting event and ν_τ analysis samples are nearly equivalent at the
128 energies where they overlap, the ν_τ optimized sample is given the highest priority. Events passing
129 the ν_τ optimized selection are treated using its topology classification scheme: For events classified
130 as single cascades and tracks, deposited energy and zenith angle are used as observables, while for
131 those classified as double cascades, tau length and decay energy observables are used. It would be
132 desirable to use the total deposited energy and direction observables for the double cascade events,
133 but it appears that doing so would involve dividing the data into too many bins for the amount of
134 simulated data currently available to provide precise model expectations in all bins. The remaining
135 events of the new, high statistics starting event sample are then included using the same observables
136 as in the analysis of that sample alone. Finally, the Earth-crossing muons are included in the fit,
137 omitting those starting muon events which were already selected by the starting sample. Muon
138 zenith angles and reconstructed muon energies are used for fitting, as in [3]. After de-duplication
139 of the input data, events are classified by topology: Single cascade, double cascade, starting track,
140 or through-going track, depending on either the topology classification of the source dataset, or by
141 treating the entire dataset as a topology category in the case of the through-going muons remaining
142 in the Earth-crossing dataset after the starting events are removed. The topology categories do not
143 all map to single neutrino flavor, nor are the classifications always correct. These limitations are
144 encompassed by the Monte Carlo simulated data, which include all neutrino flavors and interac-
145 tion process relevant in the energy range of the analysis, and which are processed and classified
146 in exactly the same manner as the observed experimental data. Furthermore, a new feature of this
147 analysis is use of a consistent set of simulated data for fitting all observations, ensuring that sys-
148 tematic effects will be accounted for in a consistent manner. This is planned to coincide with a
149 reprocessing of IceCube data over the time period to be used which will bring old data up to the
150 same standard as the most recent data-taking periods, eliminating season to season variations from
151 software changes, removing the need for complex treatment to fit these differences out.

152 The analysis fit will be performed using the same method as the starting event only analysis,
153 and as such the same model parameters will be included. However, as the primary goal of this
154 combined analysis is the flavor composition, all fits will be performed with the three flavor com-
155 ponents of the astrophysical flux allowed to float to distinct normalizations. Additionally, allowing
156 the fitted fraction of neutrinos to vary with respect to the fraction of anti-neutrinos has been ex-
157 plored using Monte-Carlo studies. While this analysis would have some ability to constrain such a
158 parameter, due to resonant W^- production by high energy $\bar{\nu}_e$ interacting with electrons in the Earth
159 (the Glashow resonance) and small changes to the absorption of the flux in the Earth due to the dif-
160 ference between neutrino and antineutrino cross sections, the sensitivity does not appear to be great
161 enough to be useful at this time, and it seems preferable to continue with the assumption of a flux
162 with equal parts neutrinos and antineutrinos and keep this degree of freedom out of the fit. Fig. 4
163 shows the projected sensitivity of this analysis using the three samples outlined above. Overall, the
164 result is similar to the expectation for the ν_τ analysis of [9], but the inclusion of the Earth-crossing
165 muons considerably reduces uncertainty on the ν_μ fraction. Fig. 5 shows the ability of this analysis

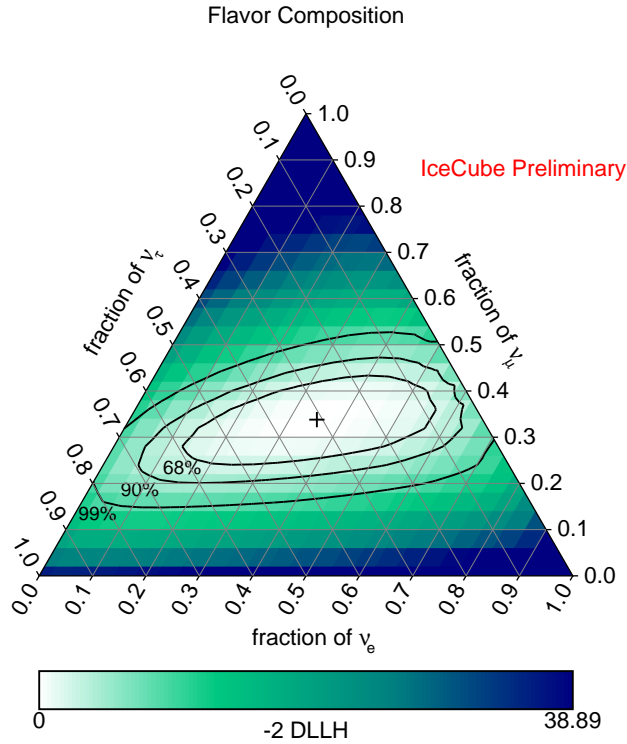


Figure 4: Median sensitivity of the global analysis to an astrophysical neutrino flux of $\Phi(E_\nu) = 1.5 \times 10^{-18} \text{ GeV}^{-1} \text{ cm}^{-2} \text{ sr}^{-1} \text{ s}^{-1} (E_\nu/100 \text{ TeV})^{-2.3}$ per flavor. This plot shows the profile likelihood space for the flavor composition with the total flux normalization allowed to float freely. The sensitivity does not change substantially for other spectra which are statistically consistent with previous observations.

166 to constrain an exponential cutoff in the astrophysical spectrum under various scenarios. A cutoff
 167 can be constrained, except for soft spectra where it becomes impossible to distinguish due to the
 168 expected number of high energy events being very small whether the cutoff is present or not.

169 5. Future Extensions

170 Besides the three samples currently integrated into the combined fit, several other data sets are
 171 complete or nearing completion which can enhance the sensitivity of this analysis. The cascade
 172 selection of [11] uses different techniques to select starting events and demonstrated to have a large
 173 fraction of events which do not appear in the starting sample offers the opportunity to substantially
 174 increase the statistics for cascade events. In addition, the selection for cascade event which are not
 175 fully contained within the detector [12] will add events not included in either of the contained event
 176 selections. Similar gains may be possible for ν_τ candidate events; [13] represents a completely dif-
 177 ferent paradigm for identifying double cascades, which is expected to have very different strengths
 178 and weaknesses, and is therefore likely to be a good complement to [9]. Finally, new veto-based
 179 techniques for selecting additional starting track events [14] may further enhance the number of
 180 astrophysical neutrinos which can be collected with highly down-going directions. As many of
 181 these data sets as possible are planned to be included to form a truly global analysis, along with

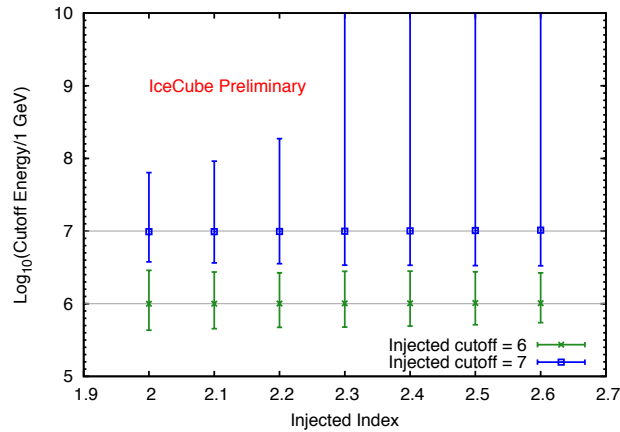


Figure 5: Median sensitivity of the global analysis to the energy of an exponential cutoff in the astrophysical neutrino spectrum. Error bars show 68% uncertainty intervals for the fitted cutoff. The extension of these intervals to energies far larger than any event expected to be observed in data for soft spectra indicates an inability to distinguish the injected cutoff from a case with no cutoff.

182 any other new selections and observables which may become available in the near future. Further-
 183 more, this type of analysis will benefit from improved calibration which will become possible with
 184 IceCube-Gen2.

185 References

- 186 [1] M.G. Aartsen et al., *Science* **342**, 1242856 (2013)
 187 [2] R. Abbasi et al., *Phy. Rev. Lett.* **111** 021103 (2013)
 188 [3] M. G. Aartsen et al., *ApJ* **833**, 1 (2016)
 189 [4] **IceCube** Collaboration, *PoS (ICRC2017)* 981 (2017).
 190 [5] M. G. Aartsen et al., *Phys. Rev. D* **91**, 022001 (2015)
 191 [6] R. Enberg, M. H. Reno, and I. Sarcevic, *Phys. Rev. D* **78** 043005 (2008)
 192 [7] M. G. Aartsen et al., *Phys. Rev. D* **89**, 062007 (2014)
 193 [8] M. G. Aartsen et al., *ApJ* **809**, 1 (2015)
 194 [9] **IceCube** Collaboration, *PoS (ICRC2017)* 974 (2017).
 195 [10] **IceCube** Collaboration, *PoS (ICRC2017)* 1005 (2017).
 196 [11] **IceCube** Collaboration, *PoS (ICRC2017)* 968 (2017).
 197 [12] **IceCube** Collaboration, *PoS (ICRC2017)* 1002 (2017).
 198 [13] **IceCube** Collaboration, *PoS (ICRC2017)* 1009 (2017).
 199 [14] K. Jero, "Enhanced Starting Track Event Selection," *Presentation at IPA Conference, May 8-10, 2017,*
 200 *Madison, WI, USA*